Iacob-Liviu SCURTU, Monica BALCĂU, Ancuța JURCO, Ioana CRĂCIUN, Andrei KIRALY, Ioan SZABO

EVALUATION AND IMPROVING THE AERODYNAMICS OF THE COMMERCIAL VAN

Abstract: *The aerodynamic evaluation of vehicles body structure represents a significant stage in a car body design, having a considerable implication in fuel reduction and an increased vehicle stability on the road. The aim of this paper is to determine the aerodynamic coefficient, illustrating the airflow streamlines around the body of a VAN and reducing the aerodynamic coefficient by adding air deflectors to the vehicle body structure. The starting point of the CFD aerodynamic study is represented by the determination of the air flow regime around the vehicle body, followed by the determination of the aerodynamic coefficient and the lift coefficient for the base model of the vehicle. In the second stage the reduction of the aerodynamic coefficient is done by adding the air deflectors in the rear side of the vehicle. The aerodynamic study is performed for each vehicle model separately, resulting three simulation cases at a 25, 35 and 45 m/s velocity. The last part of the paper presents the conclusions of the obtained results and the strong and weakness points by using the CFD simulation in vehicles aerodynamics evaluation.*

Key words: *CFD simulation, drag coefficient, drag force, Reynolds number, turbulent flow.*

1. INTRODUCTION

Lately, in Romania has been observed an increase of using the vehicle from VAN category, due to multiple product transport and lower fuel consumption compared to the truck vehicles. In our country, the VAN are mainly used in courier delivery services. The VAN is defined as a covered vehicle designed to carriage of different products and persons, larger than a regular car, but smaller than a truck. This car was designed to distribute the product quickly at the lower cost. The products distribution in the surrounding areas of the cities is carried out through these vehicles. To perform this aerodynamic study, a specific bibliography was read, including latest articles published in the vehicles aerodynamics field by using the CFD (Computational Fluid Dynamics) method analysis.

In 2016, an aerodynamic study was performed to illustrate and compare the differences of a normal operating conditions of the vehicle and the various air turbulence condition during the road vehicle running [2].

Using the k-ε turbulence model an aerodynamic study was performed on a pickup truck structure designed at 1:20 scale. The experimental simulation was performed into a wind tunnel at the air velocity range between 36-90 km/h, and the CFD simulation was solved using the Fluent software. To improve the aerodynamic performance are proposed six cases: first case with the normal box, in the second case the wildtrack accessories are added at top and the rear of the pickup cabin, in third case the box is covered, in fourth case the box are covered with a square shape, in fifth case the front grill is performed to decrease the drag coefficient and in the last case the square cover of the box are slant in the rear side. Following the study, can be observed that the drag coefficient value of the last case decreases from the normal case lowest about 0.3 [4].

The airflow around the pickup truck was studied using CFD method by Kim et all., in Star CCM+ software. The CAD model of the car was modelled in SolidWorks in three configurations. The first configuration represents the base configuration of the pickup truck, in the second case on the base configuration are added a tailgate spoiler and in the third case the cabin roof is tapered. The simulations are performed at 30, 50, 70 mph velocity. The results shows that the model with tailgate spoiler has an improvement almost 2.95% compared to baseline truck model at 50 mph, and with 14.35% at the tapered cab roof model at 70 mph velocity [1].

In this paper, the aerodynamic study of the Dacia Dokker car model was performed, to improve the aerodynamic performance. This vehicle model was chosen because it is manufactured in Romania, being part of the local vehicles manufacturing market.

2. WORK METHOD

In this chapter are presented the general steps to create the aerodynamic CFD study.

2.1 CAD design

The CAD model of the vehicle was designed in SolidWorks environment using the blueprints picture. The model was modelled respecting the real overall dimensions of the Dacia Dokker vehicle.

Figure 1 The CAD model of the Dacia Dokker.

In Figure 1 are presented the projection modality of the blueprints picture and the base model of the car. After modeling of the vehicle body, that is represented in triple orthogonal projection and axonometric projection using wireframe visualization modality. The overall dimension

of the car model can be observed in Figure 2. To a better similarity with a real car on the CAD model are detailed some auxiliar parts, such as: the projector lights, the doors handle, the slot of the registration number in the rear side, the mirrors, the frontal grill, etc.

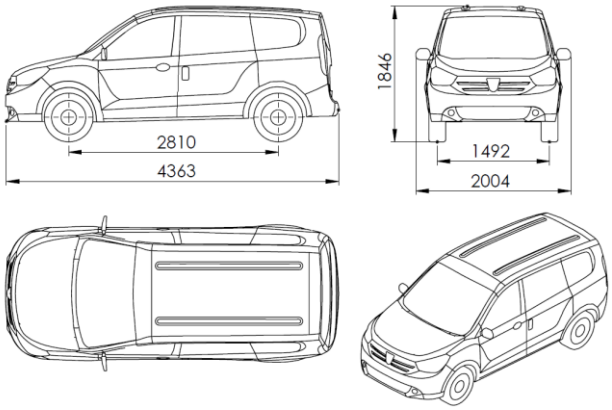

Figure 2 Car model overall dimensions.

The undercarriage part of the car is considered covered by a flat plate, without any grooves.

2.2 Forces on vehicle

During driving on the road, the air exerts a permanent force on the body care surface that makes it difficult to move forward.

The air resistance is represented by the drag force that acts parallel to the road but in opposite direction to the vehicle's forward direction. The expression of this force is presented in relation 1:

$$F_x = \frac{1}{2} \cdot \rho \cdot V^2 \cdot C_D \cdot A \qquad (1)$$

where:

F_x - drag force, ρ - air density, V - airflow velocity, C_D - drag coefficient, A - frontal area of the car.

From the drag force expression can be deducted the relation of the drag coefficient presented in relation 2:

$$C_D = \frac{2 \cdot F_x}{\rho \cdot V^2 \cdot A} \qquad (2)$$

About 55-60% of the total of the air resistance is caused by the windscreen geometry, up to 18% is determined by the protrusions located on the car's body, and up 15% is caused by the airflow through the grill radiator and the wheels space.

The force that acts on a perpendicular plane to the forward direction is lift force. This force may cause the automobile lift when is applied in a positive direction, and in case when the force act in negative direction may exert a supplementary pressure on the vehicle's wheels. In the case of negative action, the lift force will be called down force.

The expression of the lift force is written in relation 3:

$$F_y = \frac{1}{2} \cdot \rho \cdot V^2 \cdot C_L \cdot A \qquad (3)$$

where, C_L represent the lift coefficient, and his deducted expression is presented in relation 4:

$$C_L = \frac{2 \cdot F_y}{\rho \cdot V^2 \cdot A} \qquad (4)$$

In Figure 3 are illustrated the forces that acts on the vehicles body and the frontal area that are necessary to drag coefficient determination.

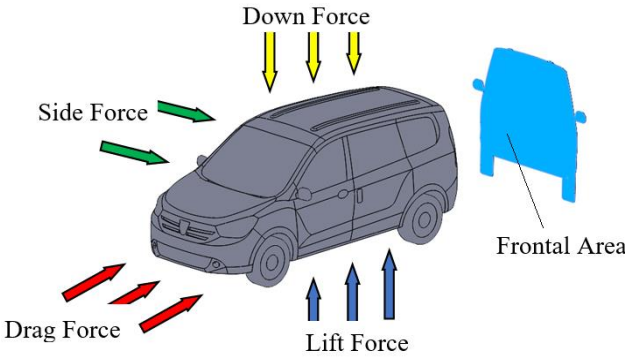

Figure 3 The force that acts on the vehicle body and the frontal area.

Another force that acts on the vehicles body is given by the wind side effect that represent the side force that acts only if the air has a lateral movement.

The expression of the lateral force is presented in the relation 5:

$$F_z = \frac{1}{2} \cdot \rho \cdot V^2 \cdot C_z \cdot A \qquad (5)$$

The expression of the side coefficient is presented in relation 6:

$$C_z = \frac{2 \cdot F_z}{\rho \cdot V^2 \cdot A} \qquad (6)$$

Due to the use of the road in this study it was not considered necessary to calculate the lift force and lift coefficient, also the lateral wind force is neglected.

2.3 Mathematical model

The mathematical model used in this paper is based on the Reynolds Averaged Navier Stokes algorithm. The standard k-ε turbulence model is used in this research. The representation in Cartesian tensor form of the equations are represented in relation 7 and 8 [6]:

$$\frac{\partial U_i}{\partial x_i} = 0 \qquad (7)$$

$$\rho = \frac{\partial}{\partial x_j}\left(U_j U_i + \overline{u_j' u_i'}\right) = -\frac{\partial P}{\partial x_i} + \frac{\partial}{\partial x_j}\left(2\mu S_{ij}\right) \qquad (8)$$

where, U_i is the mean of velocity tensor, x_i is vector position, $\overline{u_j' u_i'}$ is the average of fluctuating velocity, P is the mean static pressure, μ is the molecular viscosity.

The strain rate expression is given in relation 9:

$$S_{ij} = \frac{1}{2}\left(\frac{\partial u_i}{\partial x_j} + \frac{\partial u_j}{\partial x_i}\right) \quad (9)$$

The equation 10 represented the turbulence model k-ε.

$$\rho U_j \frac{\partial k}{\partial x_j} = \tau_{ij}\frac{\partial U_i}{\partial x_i} - \rho\varepsilon + \frac{\partial}{\partial x_j}\left[\left(\mu + \frac{\mu_T}{\sigma_k}\right)\frac{\partial \varepsilon}{\partial x_j}\right] \quad (10)$$

where, τ_{ij} is the Reynolds stress, μ_T is turbulent viscosity, σ_k is closure coefficient, k is turbulent kinetic energy and ε is dissipation rate of turbulent energy.

The next relation represents the dissipation rate of turbulence kinetic energy:

$$\rho U_j \frac{\partial \varepsilon}{\partial x_j} = C_{\varepsilon 1}\frac{\varepsilon}{k}\tau_{ij}\frac{\partial U_i}{\partial x_j} - C_{\varepsilon 1}\rho + \frac{\varepsilon^2}{k} + \frac{\partial}{\partial x_j}\left[\left(\mu + \frac{\mu_T}{\sigma_\varepsilon}\right)\frac{\partial \varepsilon}{\partial x_j}\right] \quad (11)$$

The expression of the turbulent viscosity is given in relation 12:

$$\mu_T = \rho C_\mu \frac{k^2}{\varepsilon} \quad (12)$$

2.4 Reynolds number

The airflow around the vehicle body can be determined by calculating the Reynolds number. This number was named after Osborne Reynolds, who introduced it in 1883 in fluid experiments. This is a dimensionless number that represent the ratio between the inertial to viscous forces characterizing the flow regime [3]. In this study, the flow regime was determined considering the flow over a plane surface. The expression of the Reynolds number is represented in the next relation:

$$R_e = \frac{\rho \cdot V \cdot L}{\mu} \quad (13)$$

The Reynolds number is calculated according to the relation 13 at three velocity cases, according to table 1.

Table 1

Reynolds number calculated values.

	Airflow velocity [m/s]		
	25	**35**	**45**
Re	$7.29 \cdot 10^6$	$1.02 \cdot 10^7$	$1.31 \cdot 10^7$

The calculus was performed at air density ρ=1.2041 kg/m^3, corresponding to a temperature T= 20°C, the dynamic viscosity μ=$1.802 \cdot 10^5$ kg/(m·s) and a car length L= 4.363 m. In this case the results show a transient flow regime at the first case with 25 m/s velocity, followed by a turbulent flow at 35 and 45 m/s velocity.

3. NUMERICAL SIMULATION

In this section are establish the computational domain and imposed boundary conditions to determine the aerodynamic study for base and improved model.

3.1 CFD domain

The computational domain is designed for a better view of the airflow behavior around the vehicle body. The computational domain has a width of 4 m, a heigh of 2.5 m and a length of 25 m, as can be seen in Figure 4. The front part of the vehicle is placed at 4 m of air inlet.

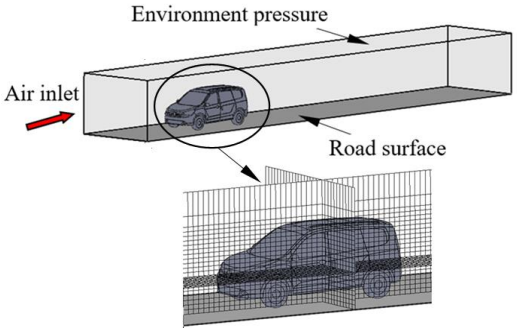

Figure 4 The CFD domain and mesh grid.

The computational volume is meshed into 129869 fluid cells, of which 12646 fluid cells are in contact with the body car surface. To increase the results accuracy and decrease the computational time the fluid layers are denser nearby the body car surface, as can be seen in detail of Figure 4. The ends of the CFD domain are bounded by the atmospheric pressure.

3.2 Boundary conditions

The aerodynamic evaluation is performed at three velocity cases: 25 m/s, 35m/s and 45 m/s. The last simulation case was chosen to be at 45 m/s because the most VANs are factory limited to this running speed. The air density is 1.2041 kg/m^3, corresponding to a 20°C temperature of the simulation environment. Also, the value of the aerodynamic force is calculated in SolidWorks.

4. RESULTS

This section presents the CFD simulation results for both model: the base and improved model. In the first part are presented the calculated values and in the second part are presented the visual results of the velocity and pressure distribution on the vehicle body.

4.1 Base model

The numerical results of the base model, of the drag force and drag coefficient are presented in table 2 for three air velocity cases. It can be observed that the values of the drag force are in range of 379.800 – 1214.970 N and the lower value of the drag coefficient is when the air velocity have 45 m/s.

Table 2

Numerical result of the base model.

Velocity	25 m/s	35 m/s	45 m/s
Drag force [N]	379.800	739.518	1214.970
Drag coefficient	0.371	0.382	0.366

Following are presented the visual results for the base model. In Figure 5 are presented the streamline behavior at 25 m/s air velocity. For a better view the graphical results are represented in all orthogonal projections and in front and rear axonometric view.

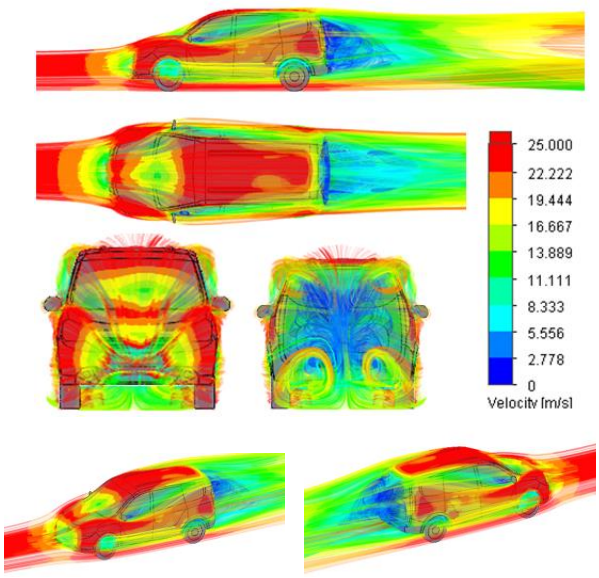

Figure 5 Air velocity distribution at 25 m/s velocity.

The largest low velocity field is created in the rear side of the vehicle and in the wheel housing, that have a negative influence to forwarding of the vehicle. Also, in the rear of the side mirror is generated a small low velocity field. In section the pictures are represented to view the behavior around the vehicle body, not including all calculation volume.

The air velocity distribution at 35 m/s is presented in Figure 6.

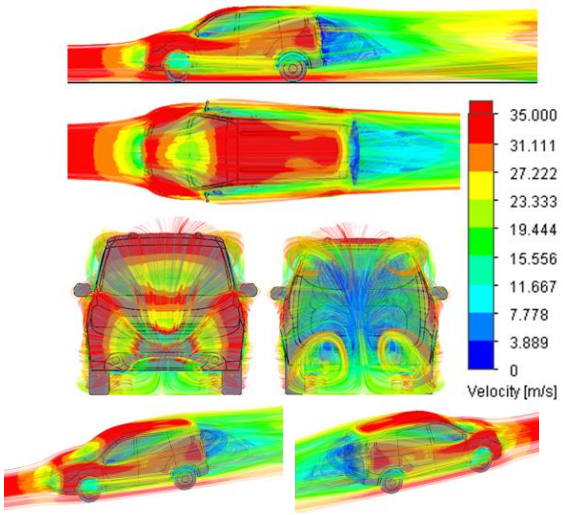

Figure 6 Air velocity distribution at 35 m/s velocity.

The results at 35 m/s is almost similar to previous case results. At a 45 m/s air velocity the visual results are better highlighted compared to previous results and the streamlines are smoother, as can be seen in Figure 7. It can be observed that the low velocity field situated in the rear side of the vehicle is smaller comparing to the results at 25 and 35 m/s.

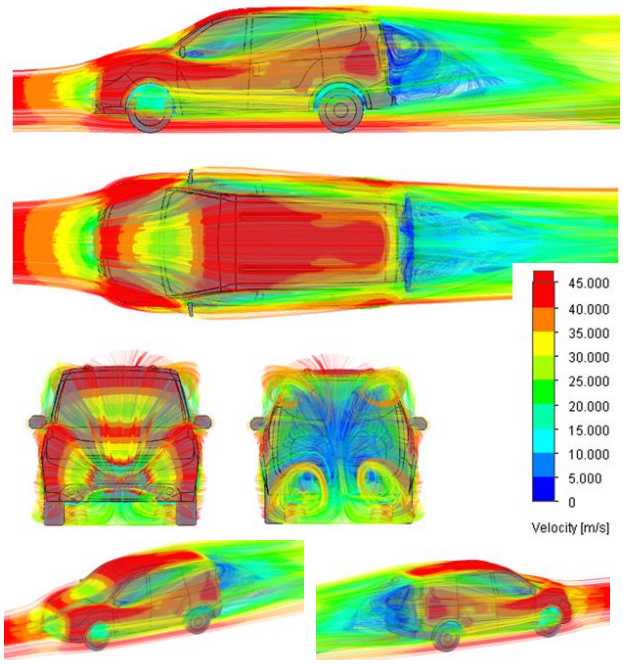

Figure 7 Air velocity distribution at 45 m/s velocity.

This aerodynamic study was performd considering the road surface. In Figure 8 is presented the airflow presure distribution on the car body surface and the road surface nearby the vehicle.

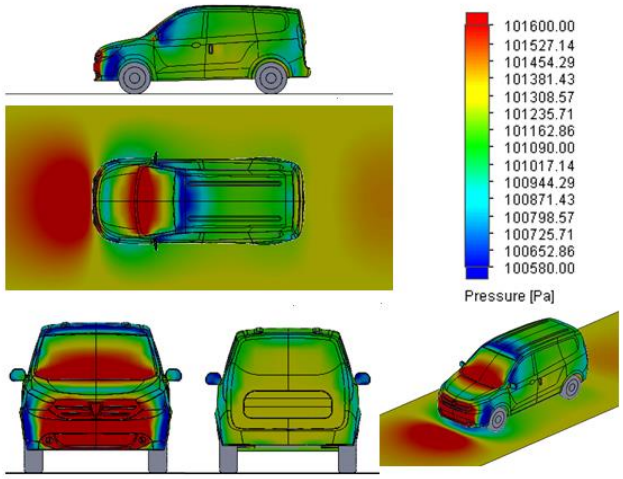

Figure 8 Air pressure distribution at 45 m/s velocity at the base model.

It can be observed that the air pressure has a maximum on the windscreen and the rear side of the bonner. Also, the maximum air pressure apear on the road surface in the front of the vehicle. A smaller

pressure surface appeares behind the car body at 1 m aproximate from this. The areas with the lower pressure are situated on the rear side mirrors, on the front roof and on the lateral surface of the frontal bumper, as can be seen in Figure 8.

4.2 Improved model

The improved model has a two modification of the base car structure. In the rear side in continuation of the car roof is added an air deflector and in the lower side are designed an air diffusor, as can be seen in Figure 9.

Figure 9 Improved elements added on cat body.

The resulted values of the drag force are in the range of 370.076 – 1183.960 N, and the lower value of the drag coefficient is 0.357 at the 45 m/s air velocity (Table 3).

Table 3

Numerical result of the improved model.

Velocity	25 m/s	35 m/s	45 m/s
Drag force [N]	370.076	721.448	1183.960
Drag coefficient	0.361	0.359	0.357

The airflow behavior at a 25 m/s velocity is presented in Figure 10, where can be observed that the low velocity volume formed in the rear side of the car body are smaller having a sharper shape compared to the results of the base model.

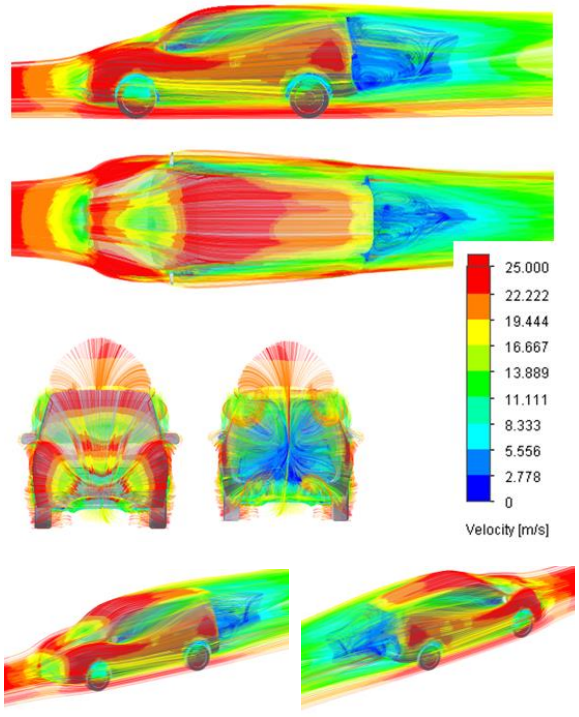

Figure 10 Air velocity distribution of the improved model at 25 m/s velocity.

The air velocity distribution of the improved model at 35 m/s velocity is presented in Figure 11.

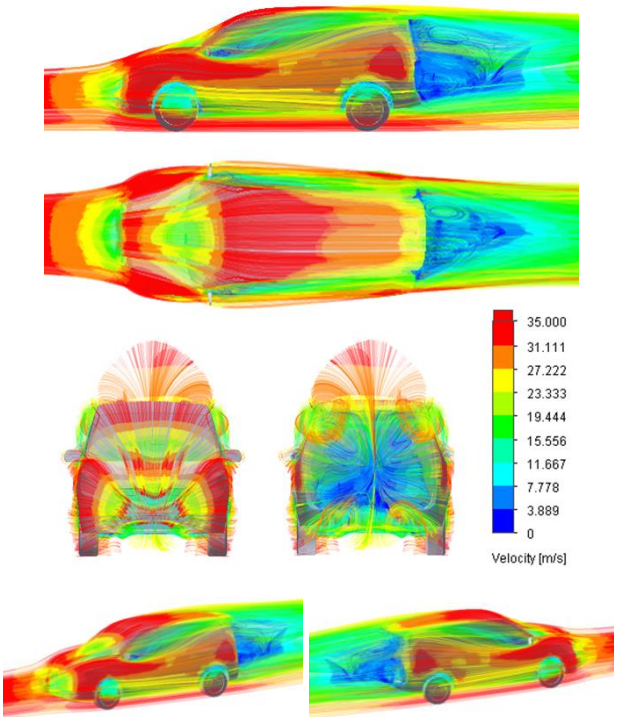

Figure 11 Air velocity distribution of the improved model at 35 m/s velocity.

In Figure 12 is presented the airflow distribution around the car body.

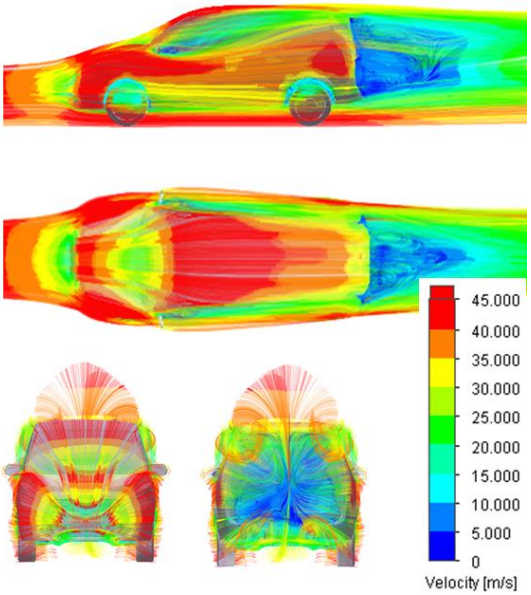

Figure 12 Air velocity distribution of the improved model at 45 m/s velocity.

It can be observed that at the streamline distribution of the improved model are oriented by the air deflector on the upper side of the car body, as can be seen in figures 10, 11 and 12. This air orientation can be viewed just in front and rear side of the car, because this effect arises at a bigger distance from the rear side of the car.

In Figure 13 the pressure distribution on the car body surface is presented. Comparing to the results from the base model it can be observed that the pressure distribution on the rear door is better distributed.

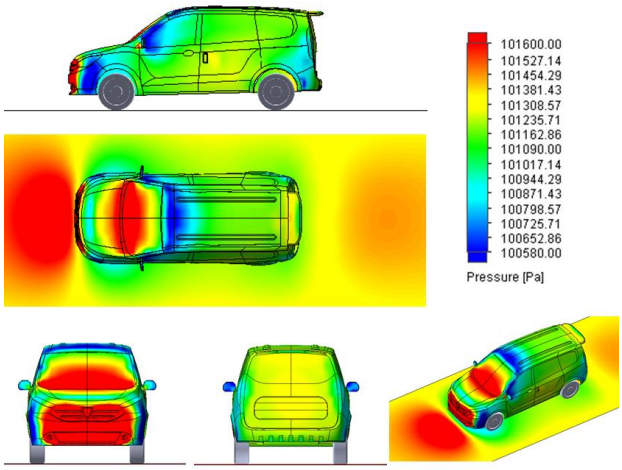

Figure 13 Air pressure distribution at 45 m/s velocity at the improved model.

5. CONCLUSIONS

In this paper, the CFD study based on numerical evaluation is determined. Comparing the obtained results at the base and the improved model, can be viewed that the lower value of the drag coefficient is resulted at the improved model at 45 m/s velocity.

A strong point in using of the simulation method is given by the different loading cases that can be applied on the same virtual models. In this simulation, the errors may occur in the results interpretation, because the vehicle is moving, while the air is fixed, and the air from computational volume have a velocity given by the user. As a future direction of research can be added an air deflector in front part of the vehicle, and a new air deflector placed vertical on the rear door.

REFERENCES

[1] Kim, J., Pattermann, J., Menon, V., & Mokhtar, W. (2011). *A CFD Study of Pickup Truck Aerodynamics.* In Proceedings of the 2011 ASEE North Central & Illinois-Indiana Section Conference.

[2] Kremheller, A., Moore, M., Le Good, G., Sims-Williams, D. B., Newbon, J., & Lewis, R. (2016). *The effects of transient flow conditions on the aerodynamics of an LCV concept using CFD and wind tunnel experiments.* Institution of Mechanical Engineers (IMechE).

[3] Ljubomir, M., Dalibor, B., Andrija, B., & Hrvoje, K. (2018). *Aerodynamic Design of a Solar Road Vehicle.* International Journal of Automotive Technology, 19(6), 949-957.

[4] Mukda, P. (2016). *Effect from Accessories on Pickup Aerodynamics by Computational Fluid Dynamics.* In 6th International Conference on Advances in Engineering Sciences and Applied Mathematics (ICAESAM'2016) (pp. 59-63).

[5] Scurtu, I. L. (2021). *Aerodynamic performance evaluation for a vehicle structure equipped with a bicycle rack.* Journal of Automotive Engineering, ISSN 2457 – 5275, Vol. 27-22, pp 5-14.

[6] Scurtu, I. L., & Gheres, M. I. (2022). *Numerical evaluation of vehicles aerodynamics in platoon using CFD simulation.* In IOP Conference Series: Materials Science and Engineering (Vol. 1220, No. 1, p. 012024). IOP Publishing.

[7] https://www.dreamstime.com/renault-dokker-stepway-passenger-van-blueprint-detailed-template-design-production-vehicle-wraps-scale-to-image 205911805. *Accessed*: 2022.03.12.

Authors:

Lecturer PhD. Eng. Iacob-Liviu SCURTU, Technical University of Cluj-Napoca, Faculty of Automotive, Mechatronics and Mechanical Engineering, Department of Automotive Engineering and Transports, E-mail: liviu.scurtu@auto.utcluj.ro

Lecturer PhD. Eng. Monica BALCĂU, Technical University of Cluj-Napoca, Faculty of Automotive, Mechatronics and Mechanical Engineering, Department of Automotive Engineering and Transports, E-mail: monica.balcau@auto.utcluj.ro

Asist. Prof. PhD. Eng. Ancuța JURCO, Technical University of Cluj-Napoca, Faculty of Automotive, Mechatronics and Mechanical Engineering, Department of Automotive Engineering and Transports, E-mail: ancuta.jurco@auto.utcluj.ro

Asist. Prof. PhD. Arh. Ioana CRĂCIUN, Technical University of Cluj-Napoca, Faculty of Automotive, Mechatronics and Mechanical Engineering, Department of Automotive Engineering and Transports, E-mail: ioana.craciun@auto.utcluj.ro

Assoc. Prof. Ph.D. Andrei KIRALY, Technical University of Cluj-Napoca, Faculty of Automotive, Mechatronics and Mechanical Engineering, Department of Automotive Engineering and Transports, E-mail: andrei.kiraly@auto.utcluj.ro

Asist. Prof. PhD. Eng. Ioan SZABO, Technical University of Cluj-Napoca, Faculty of Automotive, Mechatronics and Mechanical Engineering, Department of Automotive Engineering and Transports, E-mail: ioan.szabo@auto.utcluj.ro